Mutual regulation of CD4+ T cells and intravascular fibrin in infections

Tonina T. Mueller,[1,2*] Mona Pilartz,[1*] Manovriti Thakur,[1*] Torben LangHeinrich,[1] Junfu Luo,[1] Rebecca Block,[1] Jonathan K.L. Hoeflinger,[1] Sarah Meister,[1] Flavio Karaj,[1] Laura Garcia Perez,[3] Rupert Öllinger,[4] Thomas Engleitner,[4] Jakob Thoss,[1] Michael Voelkl,[1] Claudia Tersteeg,[5] Uwe Koedel,[6] Alexander Zigman Kohlmaier,[1] Daniel Teupser,[1] Malgorzata Wygrecka,[7] Haifeng Ye,[8] Klaus T. Preissner,[9] Helena Radbruch,[10] Sefer Elezkurtaj,[11] Matthias Mack,[12] Philipp von Hundelshausen,[13] Christian Weber,[13] Steffen Massberg,[2] Christian Schulz,[2] Roland Rad,[4] Samuel Huber,[3] Hellen Ishikawa-Ankerhold[2#] and Bernd Engelmann[1#]

[1]Institut für Laboratoriumsmedizin, Klinikum der Universität München, Ludwig-Maximilians-Universität (LMU), Munich, Germany; [2]Medizinische Klinik I, Klinikum der Universität München, LMU, Munich, Germany; [3]1. Medizinische Klinik und Poliklinik, Universitätsklinikum Hamburg-Eppendorf, Hamburg, Germany; [4]Institut für Molekulare Onkologie und Funktionelle Genomik, Technische Universität München, Munich, Germany; [5]Laboratory for Thrombosis Research, KU Leuven Campus Kulak Kortrijk, Kortijik, Belgium; [6]Neurologische Klinik, Klinikum der Universität München, LMU, Munich, Germany; [7]Center for Infection and Genomics of the Lung (CIGL), Justus-Liebig-Universität, Giessen, Germany; [8]Institute of Regenerative Biology and Medicine, Helmholtz-Zentrum München, Munich, Germany; [9]Institute of Biochemistry, Justus-Liebig-Universität, Giessen, Germany; [10]Institut für Neuropathologie, Charité - Universitätsmedizin, Berlin, Germany; [11]Institut für Pathologie, Charité - Universitätsmedizin, Berlin, Germany; [12]Medizinische Klinik II, University of Regensburg, Regensburg, Germany and [13]Institut für Prophylaxe und Epidemiologie der Kreislaufkrankheiten, Ludwig-Maximilians-Universität, Munich, Germany

**TTM, MP and MT contributed equally as first authors.*

#HI-A and BE contributed equally as senior authors.

Correspondence: B. Engelmann
Bernd.Engelmann@med.uni-muenchen.de

T.T. Mueller
Tonina.Mueller@med.uni-muenchen.de

Received: November 5, 2023.
Accepted: March 25, 2024.
Early view: April 4, 2024.

https://doi.org/10.3324/haematol.2023.284619

Supplementary Data - **Mutual regulation of CD4$^+$ T cells and intravascular fibrin in infections**

Supplementary Methods

Mouse treatments

The following antibodies were used for depletion of immune cells: CD4$^+$ T cells (αCD4 antibody, GK1.5, 500 µg/mouse, Biolegend)[1,2], neutrophils (αLy6G antibody, 1A8, 400µg/mouse, BioXCell)[3] and classical monocytes (αCCR2 antibody, 20µg/mouse)[4]. The following antibodies or chemicals were used for neutralization prior to infection: αuPA[5] (MU1; 10 mg/kg body weight, provided by Michael Ploug), αTAFI[6] (MA-RT36A3F5, 5 mg/kg body weight, both provided by Paul Declerck), carboxypeptidase inhibitor (CPI, C0279, Sigma)), αLFA-1[7] (M17/4, 100 µg/mouse, BioXCell), αMHC-II[8] (Y-3P, 500 µg/mouse, BioXCell), αIL12p40[9] (C17.8, 500 µg/mouse, BioXCell). Factor VIIa (Novoseven®, Novo Nordisk) was injected via tail vein as previously described[10].

Thrombelastometry and tpa ELISA

Blood was collected from the mice by cardiac puncture using natrium-citrate as a anticoagulant (1:10). Fresh whole blood was immediately used for analysis (<30min) after collection for optimal results. Thus, we combined 300 µl of murine whole citrate blood 20 µl of EXTEM solution (#503-05, Tem Innovations GmbH, Munich, Germany) in reagent cups (#200011, Tem Innovations GmbH) and added 20 µl of StarTEG solution (#503-10, Tem Innovations GmbH). Subsequently, we determined clotting time (CT), clot formation time (CFT), maximum clot firmness (MCF), and the alpha angle at 37 °C.

For the assessment of tpa levels, collected blood was centrifuged at 2500g for 20min at 4°C twice to collect platelet poor plasma. Plasma was added to the ELISA and preparation and measurements were performed according to manufacturer's instructions (biorbyt #orb776434) at 450nm using a plate reader.

Analysis of Kaede mice

Excitation of the photoconvertible protein Kaede with an ultraviolet laser causes the emission to change from green to red Kaede green and Kaede red cells were detected via flow cytometry by their respective fluorescence emission and Th17 cells were identified as CD45$^+$ CD3$^+$ CD4$^+$ IL-

17A$^+$. To exclude γδT cells, kaede green and kaede red cells were analyzed as CD45$^+$ CD3$^+$ CD4$^+$ TCRγδ$^+$ IL-17A$^+$ cells. Less than 15% of CD45$^+$ CD3$^+$ CD4$^+$ IL-17A$^+$ cells represented γδT cells.

CD4 Isolation

The spleen was gently smashed through a 70 µm strainer and cells were collected in MACS buffer (2 mM EDTA, 0.5% bovine serum albumin (BSA) in PBS) and pelleted afterwards (450g, 5min) at room temperature. The pellet was resuspended in cold 1x RBC lysis buffer (8.26 g NH_4Cl, 1.19 g $NaHCO_3$, 0.2 ml 0.5 M EDTA in 1l ddH_2O, pH 7.3) and incubated for 5min. The reaction was stopped by adding MACS buffer (2-3x). Cells were resuspended and passed through a filter (40 µm pore size) and diluted in MACS buffer for cell separation. CD4$^+$ T cells were isolated according to the manufacturer´s instructions (CD4$^+$ T Cell Isolation Kit, 130-104-454, Miltenyi Biotec). Before transfer of T helper cells, lymphocytes were activated in vitro using Dynabeads® CD3/CD28 according to the instructions of the manufacturer (11452D, ThermoFisher) and in some cases treated with 6-Aminocaproic acid (EACA, 10 mM, A2504, Sigma) for 2 hours. Cells were injected i.v. into mice for intravital imaging (2.5 x 10^6) or after factor VIIa-treated mice (4 x 10^6). For RNAseq experiments, plasmin formation assay and Kaede experiments, CD4$^+$ T cells or CD4$^+$IL-17A$^{Katushka+}$T cells were isolated from the liver or lung of uninfected and infected C57BL/6J mice or *kaede* x *Il17a*^{Katushka} mice by flow cytometry. Small tissue pieces of max. 5 mm size were digested for 45min at 37°C with collagenase buffer (10% heat-inactivated FBS, 1% 100× HGPG, 1 mM $CaCl_2$, 1 mM $MgCl_2$, 100 U/ml collagenase IV (Sigma), 10 U/ml DNase I (Roche) in RPMI 1640 (Gibco)), forced through a cell strainer and pelleted by centrifugation (350g, 10min, 4°C). Lymphocytes were separated using 67-40% Percoll gradient, resuspended in FACS buffer (2.5% FCS, 0.03% sodium azide, in PBS) and incubated with antibodies against CD4 (1:400, GK1.5 or RM4-5, Biolegend), CD3 (1:400, 17A2, Biolegend) and CD45 (1:200, 30-F11, Biolegend) for 20min at 4°C in the dark. Red and green Kaede cells were sorted for their IL-17A positivity.

Isolation of human CD4$^+$ T cells

Mononuclear cells were separated by Ficoll-Paque PLUS (400g, 40min, room temperature, diluted 3:1 with isolation buffer (2 mM EDTA in PBS)). Cells were washed (300g, 10min, room temperature) and centrifuged at 200g, 10min at room temperature to remove platelets. The pellet

was diluted in MACS buffer, followed by cell isolation according to the manufacturer´s instructions ($CD4^+$ T Cell Isolation Kit, 130-096-533, Miltenyi Biotec).

In vitro activation and migration of $CD4^+$ T Cells

Microscopic glass slides (Menzel SuperFrost Plus) were coated with 0.01% poly-L-ornithine (Sigma-Aldrich) for 1h at room temperature or with fibrin for 45min at 37°C. For the coating with fibrin, fibrinogen from human plasma (Sigma-Aldrich) was diluted in sterile 0.9% NaCl- solution (2.5 mg/ml) and mixed 3:1 with Thrombin (4U/ml). α-human CD3 antibody (5 µg/ml, HIT3a, Biolegend) was added to the slides and incubated for 3h at 37°C followed by washing 3x with PBS. Isolated $CD4^+$ T cells were resuspended at 1 x 10^6 cells/ml in RPMI Medium 1640 (Glutamax, 2 mM HEPES, 10% FBS, 100 U/ml penicillin, 100 mg/ml streptomycin). The cells were incubated with α-human CD28 antibody (5 µg/ml, CD28.2, Biolegend) at 37°C and 5% CO_2 in a humidified atmosphere. In some cases cells were treated with either an IgG control or an anti-human LFA-1 antibody (20 µg/ml, BioXCell).

To measure T cell migration, 10^5 T helper cells were added to the pre-treated slides and incubated for 30min to allow their tight interaction with the surface. The cells were then visualized every 5min for 3h in a visual field of 500 µm x 500 µm (37°C, 5% CO_2). To track the cell movements, the videos were analyzed using FIJI (Trackmate Plugin[11]). Both, the covered distance as well as the speed of the cells were analyzed.

Immunohistochemistry of frozen samples

All antibodies were unconjugated unless stated otherwise. Sections were stained with secondary antibody (1:1000, AF488, AF546, AF594, AF647, α-rat IgG, α-rabbit IgG, α-mouse IgG, α-goat IgG, Thermo Fisher) for 1h at 4°C. Dapi (1 µg/ml, Sigma Aldrich) or DRAQ5 (5 µM, Biolegend) were used for detection of nuclei.

The following antibodies were used to detect endothelial cells and to analyze formation of fibrin and thrombi: α-stabilin-2 (1:200, MBL), αCD31 antibody (1:50, abcam), α-fibrin IIβ chain antibody (1:200, T2G1, WAK-Chemie Medical GmbH). For analysis of intravascular fibrin deposition, the total vascular area of microvessels (≤ 20 µm diameter) and the fibrin-covered area inside the vessels were measured. Fibrin deposition was either calculated as percentage of fibrin-covered area of total intravascular area or as total amount of intravascular fibrin-covered area per

visual field. All fibrin parameters were calculated from 3 to 5 visual fields (142.7 µm x 142.7 µm) amounting to a total number of >100 analyzed vessels per mouse.

The different types of immune cells were identified by staining with antibodies against Ly6C (1:400, ER-MP20, abcam), Ly6G (1:100, 1A8, Biolegend, primary labelled AF488) or CX3CR1 (1:200, abcam). The different types of T helper cells were detected by staining with the following antibodies: αCD3 (1:100, Novus biologicals), αCD4 (1:150, Biorbyt or 1:150, bioss, AF488), αRORγt (1:100, Biorbyt), αTbet (1:100, antibodies-online), αGATA3 (1:200, 1A12-1D9, Invitrogen), αFoxp3 (1:300, Novusbio). 90.4% of $CD4^+$ cells were identified as $CD3^+$T cells. B cells were stained by using αCD19 (1:100, SouthernBiotech, FITC conjugated) and αCD5 (1:200, eBioscience Invitrogen) antibodies. Lymphocyte activation was analyzed by staining with αCD69 (1:400, R&D Systems) or αCD38 antibodies (1:100, 38C03, Invitrogen).

TF and IL-2 expressions were detected with αTF (1:250, 1H1, Genentech (Roche)) and αIL-2 antibodies (1:400, abcam), respectively. For detection of fibrinolytic mediators, αuPA (1:100, Proteintech or 901420, R&D systems), αuPAR (1:100, abcam), αplasminogen (1:100, abcam), αTAFI (1:100, LSBio) and αPAI-1 (1:100, abcam) antibodies were used. For all immunohistochemical quantifications at least 10 visual fields (142.7 µm x 142.7 µm) were analyzed for each sample. For the verification of the cellular internalization of immune complexes Z-stacks with a stepsize of 1 µm were analyzed. All immunohistochemical images were independently evaluated by two researchers.

Immunohistochemistry of human samples

Samples were fixed with 4% PFA and embedded in paraffin. Three micrometer sections were deparaffinized with ROTI-Histol (Carl Roth) for 20min and re-hydrated through graded ethanol washes. Antigen retrieval was performed with Tris-EDTA buffer (10 mM Tris base, 1 mM EDTA, 0.05% Tween 20, pH 9) for 7min at full pressure in a pressure cooker. After washing with tab water, sections were blocked with 2% BSA, 10% goat serum, 0.1% Tween-20 in TBS for 1h at room temperature and washed afterwards (3 x 3min) with TBS-T. Samples were incubated with primary antibodies (αCD4 (1:200, Bioss); αCD31 (1:100, JC/70A, abcam); αfibrin β chain (1:100, REF 350, LOXO)) for 1h at room temperature or overnight at 4°C, washed and incubated with secondary antibody for 1h at 4°C. Tissue sections were mounted with Fluoroshield Mounting Medium with Dapi (abcam).

For analysis of thrombus formation or vessel occlusion the fibrin-covered area per vessel was measured. Thrombi were defined as aggregates formed by fibrin without or with attached blood cells that obstructed blood vessels by ≥60%. Vessel occlusions were defined as vessel obstructions ≥90%. For each sample at least 50 visual fields (290 µm x 290 µm) were analyzed. All investigations were approved by the local ethics committees (Medical Faculty of Justus-Liebig University: 29/01, Charité Berlin and Medical University of Graz: 32-362ex19/20).

Confocal Microscopy

For imaging of IHC sections and in vitro ICC experiments confocal microscopy was performed as described previously [12] or with an inverted Leica SP8X WLL microscope, equipped with 405 nm laser, WLL2 laser (470 - 670 nm) and acusto-optical beam splitter at the Core Facility Bioimaging of the Biomedical Center of LMU Munich.

Multi-photon intravital imaging

$CD4^+$ T cells isolated from C57BL/6J mice were stained with 10 µM CMTPX (Invitrogen) cell tracker for 20min at 37°C in a humidified atmosphere. CMTPX-labeled $CD4^+$ T cells (2.5 x 10^6, in 200 µl sterile PBS) were i.v. injected into mice 10min after infection with *E. coli*. Mice were anaesthetized by intraperitoneal injection of midazolame (5 mg/kg body weight, Ratiopharm), medetomidine (0.5 mg/kg body weight, Pfizer), and fentanyl (0.05 mg/kg body weight, CuraMed Pharma GmbH). One liver lobe was exposed by a suction ring. FITC-Dextran (2,000 kDa, Sigma Aldrich) was injected via catheter to label the blood flow. For intravital imaging a Multiphoton TrimScope II system (LaVision BioTec) connected to an upright Olympus microscope equipped with a Ti: Sa laser Chameleon Ultra II (coherent tunable in the range 690 to 1,080 nm) was used at 800nm excitation wavelength. The emission was detected by four high sensitive GaAsP (Gallium arsenide phosphide) detectors for single beam scanning and an additional PMT detector for Dodt contrast. Single images were acquired at a depth of 20 to 30 µm with a Z-interval of 2µm. ImSpector Pro (LaVision Biotec) was used as the acquisition software. For each animal, videos were taken over 5-6h. Videos were analyzed using Imaris 9.6.0 (Bitplane, Zurich). Migrating of $CD4^+$ T cells was defined as a movement with a speed between 0.1 µm/s and 1.0 µm/s and an average velocity below 0.35 µm/s. Tracking was performed from the beginning to the end of the locomotion sequence within a video.

Flow Cytometry

Blood was drawn by cardiac puncture and red blood cell lysis was performed. Cells were washed and stained using antibodies against CD45 (biolegend, 30-F11, PerCPCy5.5), CD3 (biolegend, 17A2, APC), CD4 (biolegend, RM4-5, PE), Ly6G (biolegend, 1A8, BV711). Dead cells were stained using Fixable Viability Kit (Zombie, NIR, biolegend) according to manufacturer's instruction. Samples were acquired using an LSR Fortessa Flow Cytometer (BD Biosciences) and analyzed using FlowJo (BD Biosciences).

RNA Sequencing

In contrast to [13], the P5 and P7 sites were exchanged to allow sequencing of the cDNA in read1 and barcodes and UMIs in read2 to achieve better cluster recognition. The library was sequenced on a NextSeq 500 (Illumina) with 67 cycles for the cDNA in read1 and 16 cycles for the barcodes and UMIs in read2. Data were processed using the published Drop-seq pipeline (v1.12) to generate sample- and gene-wise UMI tables [14]. For mapping raw sequencing data reference genome (GRCm38) was used for alignment. Transcript and gene definitions were used according to the GENCODE Version M25. The resulting UMI filtered count matrix was imported into R v3.4.4. Prior differential expression analysis with DESeq2 v1.18.1 (10.1186/s13059-014-0550-8), dispersion of the data was estimated with a parametric fit using the time point as explanatory variable. The Wald test was used for determining differentially regulated genes between different time points. Shrunken log2 fold changes were calculated afterwards. A gene was determined to be differentially regulated if the absolute apeglm shrunken log2 fold change was at least 1 and the adjusted p-value was <0.01. Rlog transformation of the data was performed for visualization and further downstream analysis.

To further investigate the function of T helper cells as coagulation regulators in the context of systemic infection, an unbiased cluster analysis was performed with all significantly altered (adjusted p-value <0.05) genes. This was performed using the bioinformatics database DAVID Huang et al., 2009) by comparing the significantly altered genes with the following defined categories: KEGG Pathway, Gene Ontology Term Biological Process, and the functional categories Biological Process, Cellular Components, and Molecular Function. Subsequently, clusters were created automatically with medium stringency.

Statistical information

All statistical analyses were performed using GraphPad Prism 9 (GraphPad Software). The mean values are given ± s.e.m. The results were compared by unpaired two-tailed t-test, One- or Two-way ANOVA with Tukey's, Sidak's or Dunnett's *post hoc* tests. To test the groups of data for normality the D'Agostino-Pearson omnibus normality test was used. In case of non-normal distributions of data, a Mann-Whitney test was performed instead of unpaired two-tailed t-test. Correlation was determined by Pearson's correlation coefficient in case of normality. Unless otherwise described, all n-values given refer to separate experiments (biological replicates) performed on different animals or independent cell preparations. P values < 0.05 were considered significant.

Data availability

The data that support the findings of this study are available from the corresponding author upon request.

1. Moynihan KD, Opel CF, Szeto GL, et al. Eradication of large established tumors in mice by combination immunotherapy that engages innate and adaptive immune responses. Nat Med 2016;22(12):1402–1410.

2. Klarquist J, Cross EW, Thompson SB, et al. B cells promote CD8 T cell primary and memory responses to subunit vaccines. Cell Rep 2021;36(8):109591.

3. Boivin G, Faget J, Ancey P-B, et al. Durable and controlled depletion of neutrophils in mice. Nat Commun 2020;11(1):2762.

4. Mack M, Cihak J, Simonis C, et al. Expression and Characterization of the Chemokine Receptors CCR2 and CCR5 in Mice. J Immunol 2001;166(7):4697–4704.

5. Lund IK, Jögi A, Rønø B, et al. Antibody-mediated Targeting of the Urokinase-type Plasminogen Activator Proteolytic Function Neutralizes Fibrinolysis in Vivo. J. Biol. Chem. 2008;283(47):32506–32515.

6. Hillmayer K, Vancraenenbroeck R, De Maeyer M, Compernolle G, Declerck PJ, Gils A. Discovery of novel mechanisms and molecular targets for the inhibition of activated thrombin activatable fibrinolysis inhibitor. J. Thromb. Haemost. 2008;6(11):1892–1899.

7. Wang Y, Li D, Nurieva R, et al. LFA-1 Affinity Regulation Is Necessary for the Activation and Proliferation of Naive T Cells. J. Biol. Chem. 2009;284(19):12645–12653.

8. Stefanová I, Dorfman JR, Germain RN. Self-recognition promotes the foreign antigen sensitivity of naive T lymphocytes. Nature 2002;420(6914):429–434.

9. Chiba S, Baghdadi M, Akiba H, et al. Tumor-infiltrating DCs suppress nucleic acid–mediated innate immune responses through interactions between the receptor TIM-3 and the alarmin HMGB1. Nat Immunol 2012;13(9):832–842.

10. Massberg S, Grahl L, von Bruehl M-L, et al. Reciprocal coupling of coagulation and innate immunity via neutrophil serine proteases. Nat Med 2010;16(8):887–896.

11. Tinevez JY, Perry N, Schindelin J, et al. TrackMate: An open and extensible platform for single-particle tracking. Methods 2017;11580–90.

12. von Brühl ML, Stark K, Steinhart A, et al. Monocytes, neutrophils, and platelets cooperate to initiate and propagate venous thrombosis in mice in vivo. J. Exp. Med. 2012;209(4):819–835.

13. Parekh S, Ziegenhain C, Vieth B, Enard W, Hellmann I. The impact of amplification on differential expression analyses by RNA-seq. Sci. Rep.;6.

14. Macosko EZ, Basu A, Satija R, et al. Highly parallel genome-wide expression profiling of individual cells using nanoliter droplets. Cell 2015;161(5):1202–1214.

15. Huang DW, Sherman BT, Lempicki RA. Bioinformatics enrichment tools: paths toward the comprehensive functional analysis of large gene lists. Nucleic Acids Res 2009;37(1):1.

16. Huang DW, Sherman BT, Lempicki RA. Systematic and integrative analysis of large gene lists using DAVID bioinformatics resources. Nat. Protoc. 2009 4:1 2008;4(1):44–57.

Supplementary Fig. 1 **T helper cell subtypes and fibrin homeostasis in systemic infection**

A,**D**, T helper cell subsets in the liver microcirculation (**A**) and association of uPA with different subsets (**D**) (*E. coli*, 1h). **B**, Kinetics of intravascular fibrin deposition after *E. coli* infection. **C**, Clotting time, clot formation time, medium clot firmness and alpha angle measured by thrombelastometry in murine whole blood in uninfected (0h) and infected (3h) mice. **D,** tpa levels in murine plasma in uninfected (0h) and infected (3h) mice. **E**, Percentage of $CD4^+$ T cells of $CD45^+$ leukocytes in the blood of mice treated with αCD4 or control antibody (3h after infection). **F**, AST and ALT serum levels in the blood of uninfected mice as well as in infected mice treated with αCD4 or control antibody (3h). Dots represent different animals (**A**,**C-E**,**G**) or different visual fields in at least 3-9 animals per group (**B**). Data given as means ± s.e.m (**A**,**C-E**,**G**). P-value calculated by One-way ANOVA (**A**,**B**,**E**) or unpaired two-tailed t-test (**D**). *P <0.05, **P <0.01, ***P <0.001, ****P <0.0001.

Supplementary Fig. 2 **Differential effects of innate immune cells vs. $CD4^+$ T cells on fibrin deposition**

A,**B** Microvascular fibrin deposition in the liver after depletion of neutrophils (αLy6G, 3h, **A** left), classical monocytes (αCCR2, 1h, **A**, right) or T_{regs} (αCD25, 3h, **B**). **C**, Plasmin formation by isolated human T helper cells obtained from 3 different human donors. **D,** Fold change in microvascular fibrin deposition in the liver after injection of activated $CD4^+$ T cells, FVIIa and infection with *E. coli* (3h). Red line indicates fibrin deposition in FVIIa treated mice without $CD4^+$ cell injection. Dots represent different animals (**A**,**B**,**D**) or different donors (**C**). Data given as means ± s.e.m (**A**,**C**,**D,F**). P-value calculated by One-way ANOVA (**A-C**,**G**) or unpaired two-tailed t-test (**F,H**). *P <0.05, **P <0.01, ****P <0.0001.

Supplementary Fig. 3 **T cell arrest and activation at the peak of fibrin formation**

A,**B** Microvascular fibrin deposition in *f12*$^{-/-}$ mice (**A**) and after rivaroxaban treatment of WT mice (3h, *E. coli*) (**B**). **C**, Arrested $CD4^+$ T cells and RORγt$^+$ cells in the liver microcirculation after treatment with rivaroxaban. **D**, Heatmap showing mRNA expression levels of T helper cell

genes implicated in T cell activation (GO: 0042110) of uninfected (0h) or infected mice (3h, 18h). **E,** CD69 expression of T helper cells in a thrombus in the macrovasculature (3h). **F,** Percentage of T helper cells that are positive for fibrin, CD69 and IFNγ. Dots indicate different animals (**A-C,F**). Data shown as means ± s.e.m. P- values calculated by unpaired two-tailed t-test (**A-C,F)**.*P <0.05, **P <0.01, ***P <0.001.

Supplementary Fig. 4 **Origin of liver-associated T helper cells**

A, The small intestine of *kaede x Il7a*^{kat} transgenic mice was exposed to UV light, *E. coli* were injected i.v. and liver and lung were harvested. **B**, Kaede red- and green-emitting cells were sorted via flow cytometry for IL-17A^{+} cells and IL-17A^{-} cells in the liver (left) and lung (right). Dots indicate different animals . Data given as means ± s.e.m. P-value calculated by unpaired two-tailed t-test . *P <0.05.

Supplementary Fig. 5 **Regulation of fibrin homeostasis and LFA-1 dependent activation of CD4^{+} T cells**

A, Effect of rivaroxaban treatment on unidirectional migration of T helper cells 1-6h after infection with *E. coli* analyzed by multi-photon intravital microscopy. **B,** Percentage of IFNγ^{+} T helper cells either fibrin positive or negative in αLFA-1 treated mice. **C,** Effect of αLFA-1 antibody on plasmin formation by resting (Trest) or activated (Tact) human CD4^{+} T cells. Dots indicate different animals (**B**), different donors (**C**) or different videos of 3 animals per group (**A**). A minimum of 3 biological replicates was analyzed. Data shown are means ± s.e.m. P-values were calculated by Two-way ANOVA (**B**) or One-way ANOVA (**C).** *P <0.05, **P <0.01, *** P <0.001, ****P <0.0001.

Supplementary Fig. 6 **Thrombotic vessel occlusions in patients with SARS-CoV-2 and influenza virus infections**

A, Patient characteristics **B**, Number of thrombi and vessel occlusions in lungs of patients infected with influenza virus or SARS-CoV-2. Data are means ± s.e.m.. P-values calculated by unpaired two-tailed t-test (**B**). *P <0.05.

Supplementary Videos

Supplementary Video S1 Intravital imaging of T helper cell movements in the liver microcirculation during infection

Intravital multi-photon microscopy of the liver microcirculation of mice infected with *E. coli* (1h-6h). Representative video of experiments on 3 different mice. Videos show representative unidirectional migration and backward-forward movements of $CD4^+$ T cells. $CD4^+$ T cells (CMPTX, red), blood flow (FITC-dextran, green), Kupffer cells (autofluorescence, white/grey). Bar, 10 μm. Videos related to Extended Fig. 4**A**,**B**.

Supplementary Video S2 Effect of LFA-1 neutralization on intravascular migration of $CD4^+$ T cells

Intravital multi-photon microscopy of the liver microcirculation of *E. coli*-infected mice treated with αLFA-1 antibody or control antibody (1h-6h). Representative video of experiments on 3 different mice per group. $CD4^+$ T cells (CMPTX, red), blood flow (FITC-dextran, green), Kupffer cells (autofluorescence, white/grey). Bar, 50 μm. Videos related to Fig. 4**C**.

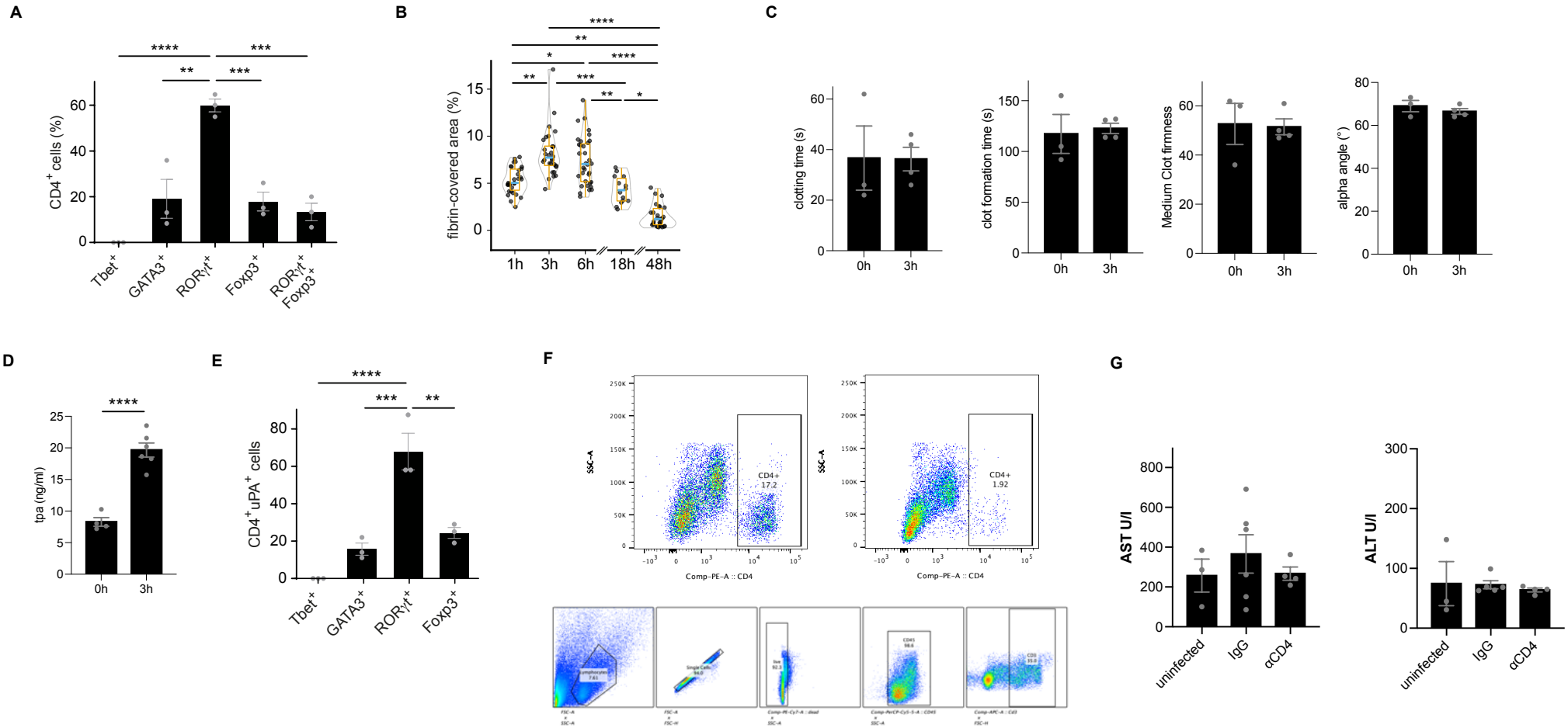

Supplementary Figure 1

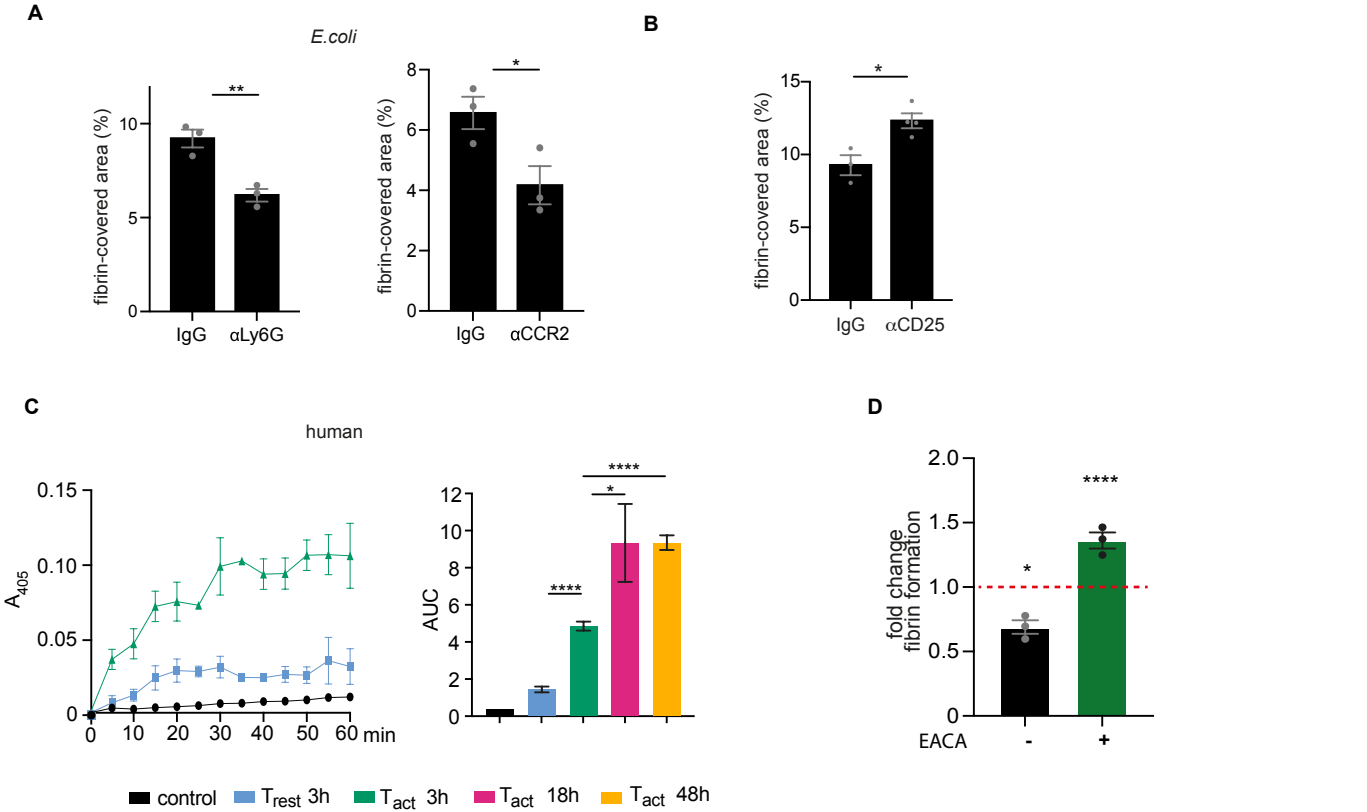

Supplementary Figure 2

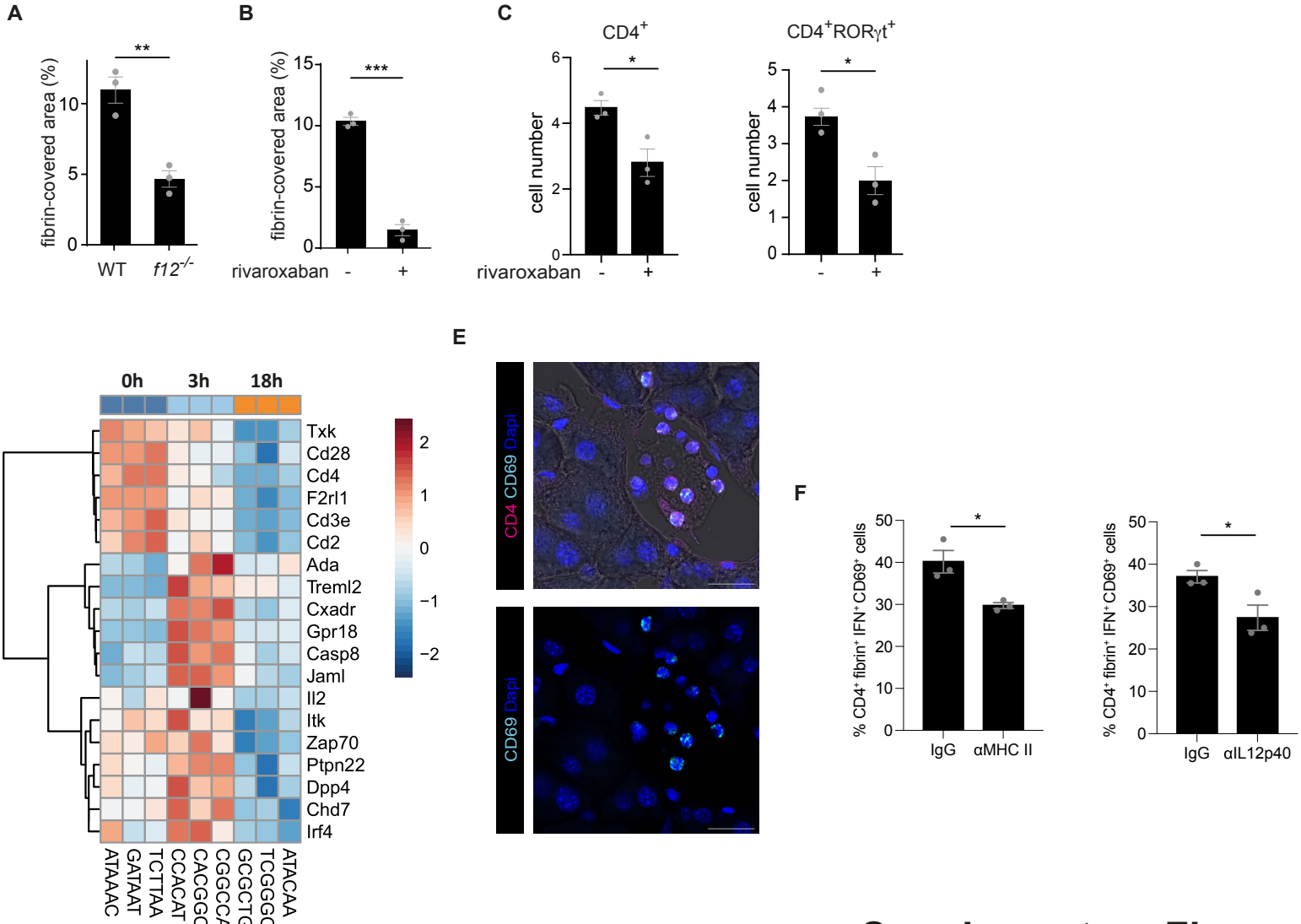

Supplementary Figure 3

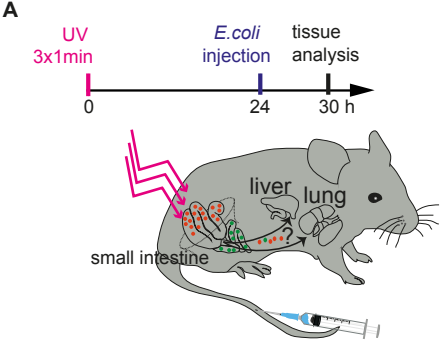

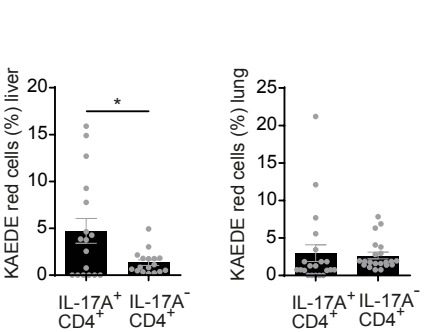

Supplementary Figure 4

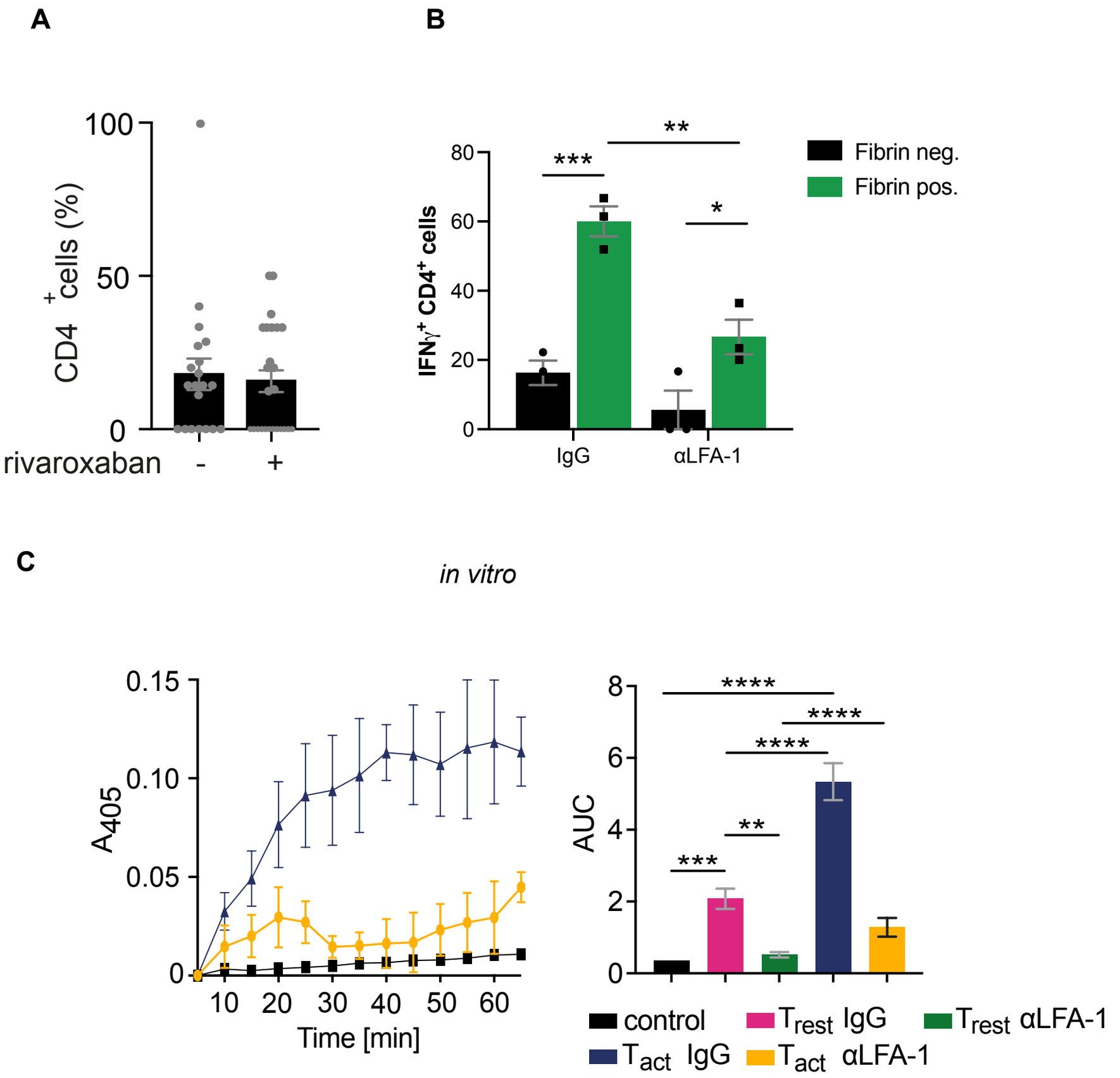

Supplementary Figure 5

A

patient	cohort	sex	age	BMI	active cancer	ECMO	catecholamine requirement
1	Covid-19	female	80	25.5	no	no	yes
2	Covid-19	female	81	*	no	no	no
3	Covid-19	male	83	23	no	no	yes
4	Covid-19	male	79	32	yes	no	no
5	Covid-19	male	85	27.2	no	no	no
6	Covid-19	female	92	24	no	no	yes
7	Covid-19	female	71	27	no	no	yes
8	Covid-19	male	77	35	no	no	yes
9	Covid-19	male	71	23	no	no	yes
10	Covid-19	male	65	42	no	no	no
11	Covid-19	female	93	28	no	no	yes
12	Covid-19	male	67	26	no	no	no
13	Influenza	female	74	33	no	no	yes
14	Influenza	female	81	26	no	no	yes
15	Influenza	female	65	39	no	no	yes
16	Influenza	male	90	21	no	no	yes
17	Influenza	male	61	23	no	no	no
18	Influenza	male	78	24	no	no	yes
19	Influenza	male	43	24.6	no	yes	no
20	Influenza	male	53	*	no	yes	yes

B

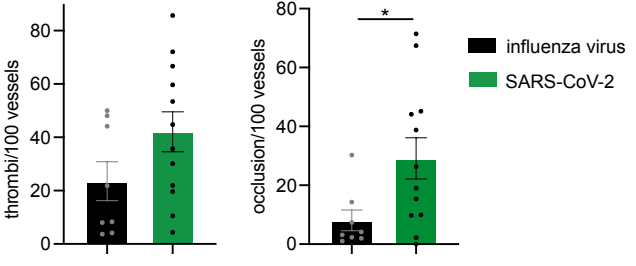

Supplementary Figure 6